The Ultimate Black Hole as a Fractal Cosmological Model: A Proof of Concept with Supernova Data

Juergen Schreiber *

Posted Date: 14 October 2025

doi: 10.20944/preprints202510.0876.v2

Keywords: ultimate black hole; fractal horizon and entropy growth; supernovae; statistics; Hubble tension

Article

The Ultimate Black Hole as a Fractal Cosmological Model: A Proof of Concept with Supernova Data

Juergen Schreiber

Independent Researcher, Dresden, Germany; juergen@schreiber.de

Abstract

We present the **Ultimate Black Hole (UBH) cosmology** as a fractal and entropic alternative to the ΛCDM paradigm. In this scenario, the Universe originates from the fragmentation of an Ultimate Black Hole, producing a self-similar distribution of smaller black holes and scale-dependent entropy growth. The resulting expansion law modifies the Hubble function in a testable way. Using the Pantheon Type Ia supernova dataset, we directly fit the UBH expansion model to the luminosity–distance relationship. For the high-redshift range ($z = 500$–1089.92), the modified Hubble function is calibrated against the ΛCDM prediction but using the same Hubble constant, $H_0 = 73\,\mathrm{km\,s^{-1}\,Mpc^{-1}}$. This unified value successfully reproduces both the local supernova observations and the CMB-derived expansion rate, thereby resolving the long-standing Hubble tension. For the 1048 supernovae, the UBH model achieves a lower χ^2 and RMS scatter than ΛCDM, with reduced χ^2 values close to unity. Standard robustness checks (clipping, jackknife, bootstrap, and MCMC calibration) confirm that the improvement is not due to outliers or calibration bias. Information criteria further favour UBH despite its larger parameter set, indicating genuine descriptive power. Our results establish UBH as a statistically competitive and physically motivated alternative to ΛCDM. By linking fractal entropy growth, Buchert's backreaction, the Fractal Early Energy term, and the curvature window, the model offers a natural resolution of the entropy paradox in cyclic cosmology and a coherent reconciliation of early- and late-universe expansion. These findings motivate further tests with upcoming multi-probe datasets.

Keywords: ultimate black hole; fractal horizon and entropy growth; supernovae; statistics; Hubble tension

List of Symbols

Table 1. Principal quantities and parameters used in the UBH cosmological model.

Symbol	Meaning
$H(z)$	Hubble function at redshift z
H_0	Present Hubble constant
Ω_m	Matter density parameter
Ω_r	Radiation density parameter
$\Omega_{k,\mathrm{eff}}(a)$	Effective curvature contribution ("curvature window")
$\Omega_{\mathrm{FEE}}(a)$	Fractal Early Energy (entropy-driven early component)
$Q(z)$	Buchert backreaction term replacing dark energy
Q_0, γ	Present amplitude and scaling exponent of $Q(z)$
$D_f(z)$	Effective mass–fractal dimension
$D_{f,\infty}$	Primordial (high-z) fractal dimension after UBH burst
β	Steepness parameter of fractal dimension evolution
a	Scale factor, $a = (1+z)^{-1}$
$a_{c,k}, \sigma_k$	Center and width of curvature window
$a_{c,\mathrm{FEE}}$	Transition scale of fractal early energy
f_{peak}	Amplitude parameter of $\Omega_{\mathrm{FEE}}(a)$
$\chi(z)$	Comoving distance, $\chi(z) = c\int_0^z dz'/H(z')$
$S_k(\chi)$	Curvature–dependent distance function
$D_A(z)$	Angular-diameter distance
$D_M(z)$	Transverse comoving distance
$d_L(z)$	Luminosity distance, $(1+z)D_M(z)$
$r_s(z_*)$	Comoving sound horizon at recombination
θ_*	Acoustic angle at recombination
M	Absolute magnitude calibration of SN-Ia sample
ΔM	Offset between observed and theoretical magnitudes
c	Speed of light

 doi:10.20944/preprints202510.0876.v2

1. Introduction

Modern cosmology faces persistent tensions between early- and late-time measurements of the cosmic expansion rate [1,2]. While the ΛCDM model successfully describes most large-scale observations, it relies on the assumption of homogeneity and a dark energy component with constant equation of state. The resulting framework reproduces the CMB anisotropies and baryon acoustic oscillations (BAO), yet shows growing discrepancies in the Hubble constant H_0 and the detailed shape of $H(z)$ inferred from supernovae and cosmic chronometers.

An alternative viewpoint emerges if one relaxes the assumption of large-scale smoothness. Inhomogeneities can modify the averaged cosmic dynamics through non-linear backreaction terms [3], while gravitational clustering itself may produce fractal-like matter distributions at different epochs [4,5]. Within this broader context, the *Ultimate Black Hole* (UBH) cosmology proposes that the Universe originated from the fragmentation of an ultimate black hole, whose decay generated a self-similar, entropy-driven hierarchy of black holes across scales. This fractal inheritance governs the expansion history through a redshift-dependent effective spatial dimension $D_f(z)$, linking microstructure, entropy growth, and large-scale kinematics.

The present paper develops this scenario into a quantitative cosmological model and performs its first observational test. By incorporating both fractal entropy effects and Buchert-type backreaction, the UBH framework generalizes the Friedmann equation while retaining a minimal, physically interpretable parameter set. Fitting this model to the Pantheon Type Ia supernova sample yields an excellent agreement and reproduces the locally measured $H_0 = 73\ \mathrm{km\,s^{-1}\,Mpc^{-1}}$, while maintaining consistency with the early-Universe calibration from *Planck*. Hence, the long-standing *Hubble tension* can be alleviated within a single, self-consistent formalism.

The structure of the paper is as follows. Section 2 outlines the theoretical foundations, introducing the fractal entropy concept, the modified Hubble function with backreaction, and the early-time FEE and curvature-window terms. Section 2.7 presents the dataset and fitting method. Section 3 summarizes the statistical outcomes and robustness tests. Section 4 discusses the physical interpretation and implications for cosmic structure, entropy evolution, and the Hubble tension. Conclusions are drawn in Section 5.

2. Theoretical Framework and Methods

2.1. Fractal Horizon Concept, Entropy Scaling, and Critical UBH Mass

A defining feature of the Ultimate Black Hole (UBH) scenario is that the horizon of a sufficiently massive black hole cannot remain a smooth, two-dimensional sphere as in the standard Bekenstein–Hawking picture [6,7]. Because the mean density decreases with increasing black-hole mass and the effective surface tension of the horizon (cf. Figure 1, [8]), the horizon of an ultra-massive object becomes limp and susceptible to deformations driven by quantum gravitational fluctuations. Such surface evolution often displays fractal characteristics, as known from natural growing processes [9].

 doi:10.20944/preprints202510.0876.v2

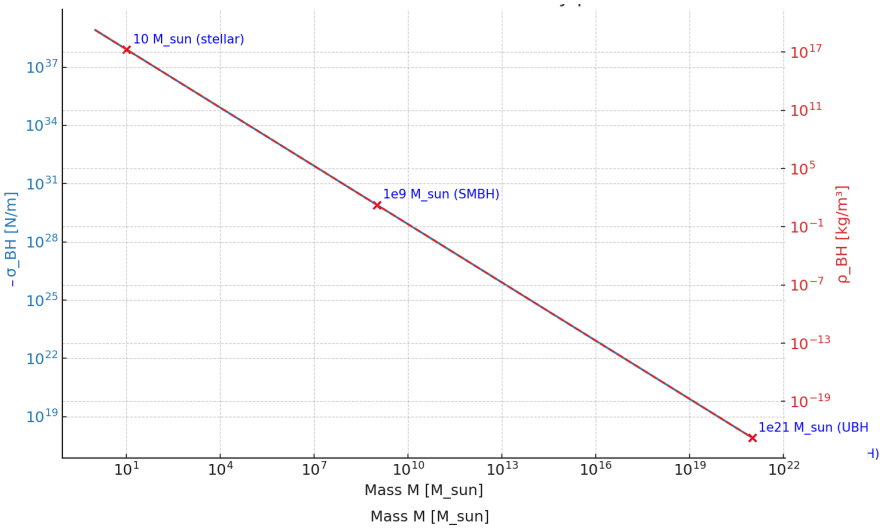

Figure 1. Mean mass density inside the Schwarzschild radius as a function of black-hole mass, $\bar{\rho}(M) = 3M/(4\pi R_s^3) \propto M^{-2}$ with $R_s = 2GM/c^2$, extended up to the UBH-relevant scale $\sim 10^{21} M_\odot$. Similar decay was found for horizon surface tension $\sigma_{\rm BH} = -1/16\pi GM_{\rm UBH}$. The steep decline of implies a weakening effective surface tension for ultra-massive horizons, making them more susceptible to macroscopic deformations and, ultimately, fractalization.

Applying this idea to the UBH horizon as a physically realistic fractal surface bounded from below by the Planck length ℓ_p and from above by a characteristic upper scale dR of the fractal fluctuations, the effective area $A_{f,h}$ of the UBH horizon scales approximately as

$$A_{f,h} \simeq A_{0,h} \left(\frac{d_R}{\ell_p}\right)^{H_h}, \tag{1}$$

where $A_{0,h} = 4\pi R_h^2$ is the area of a smooth horizon of radius $R_h = 2GM_{\rm UBH}/c^2$ and the fractal morphology of the UBH horizon is characterized by the Hurst parameter H_h with fractal dimension

$$D_{f,h} = 2 + H_h, \tag{2}$$

If the Bekenstein–Hawking relation remains valid for such a fractalized surface, the entropy of the UBH becomes

$$S_{\rm UBH,f} \simeq \left(\frac{d_R}{\ell_p}\right)^{H_h} S_{\rm UBH}, \qquad S_{\rm UBH} = \frac{4\pi k_B G}{\hbar c} M_{\rm UBH}^2, \tag{3}$$

where $S_{\rm UBH}$ is the standard entropy of a smooth-horizon black hole.

We assume that the fractal dimension $D_{f,h}$ grows with mass beyond a critical threshold M_0, for instance via

$$D_{f,h}(M_{\rm UBH}) = 3 - \exp\left[-\alpha \frac{M_{\rm UBH} - M_0}{M_0}\right], \tag{4}$$

with α a dimensionless parameter. As $M_{\rm UBH} \to \infty$, the horizon dimension saturates at $D_{f,h} \to 3$, corresponding to a fully space-filling surface.

For consistency with the second law of thermodynamics, the entropy $S_{\rm after}$ of the post-burst Universe (photons, baryons, primordial black holes, gravitational waves) must exceed the horizon entropy $S_{\rm UBH,f}$. We postulate that the fractal character of the horizon is inherited by the cosmic medium, with a fractal space Hurst parameter H_s, leading to

$$S_{\rm after} \simeq S_{\rm BH}^{\rm sum} \left(\frac{R_c}{\ell_p}\right)^{H_s}, \tag{5}$$

where R_c is the macroscopic cutoff of the fractal cosmic domain and $S_{\rm BH}^{\rm sum}$ the sum of entropies of the resulting population of black holes. Assuming $H_s = H_h$ ensures continuity of fractal properties across the UBH burst.

 doi:10.20944/preprints202510.0876.v2

The ratio of post-burst to horizon entropy is then

$$\frac{S_{\rm after}}{S_{\rm UBH,f}} = \frac{S_{\rm BH}^{\rm sum}}{S_{\rm UBH}} \left(\frac{R_c}{d_R}\right)^{H_s}, \tag{6}$$

which shows that the condition $S_{\rm after} > S_{\rm UBH,f}$ is naturally satisfied for plausible parameter choices, as it is shown in Figure 2. Inserting representative values ($M_0 \sim 10^{19} M_\odot$, $\alpha \sim 0.01$, log-normal mass distribution of primordial black holes), we find a critical UBH mass

$$M_{\rm UBH,c} \simeq 10^{21} M_\odot, \qquad R_{\rm UBH} \simeq 0.34\,{\rm Gly}, \tag{7}$$

with corresponding fractal horizon dimension $D_{f,h}^{\rm crit} > 2.656$.

The nascent fractal universe then begins with an effective spatial dimension

$$D_f^{\rm space} = 1 + H_s \simeq 1.656, \tag{8}$$

and evolves toward a three-dimensional structure during cosmic expansion.
[1]

This fractal inheritance principle sets the initial conditions for the UBH cosmology and provides a natural mechanism for entropy increase consistent with the second law and reminiscent of the cyclic conformal framework proposed by Penrose [11,12].

The redshift dependence of the effective mass–fractal dimension will be described by a smooth one–parameter relation

$$D_f(z) = 3 - (3 - D_{f,\infty}) \frac{\exp\left[\beta \frac{z}{1+z}\right] - 1}{\exp(\beta) - 1}, \tag{9}$$

with the steepness parameter $\beta > 0$. This form ensures $D_f(z \to 0) \to 3$ and $D_f(z \to \infty) \to D_{f,\infty}$. That means, in the framework of the present model the fractal universe will start its life with a fractal dimension $D_{f,\infty} = D_f^{\rm space} \simeq 1.656$ to strive during cosmic evolution after the UBH-Big-Pang towards a state with a three-dimensional structure, as we see it today.

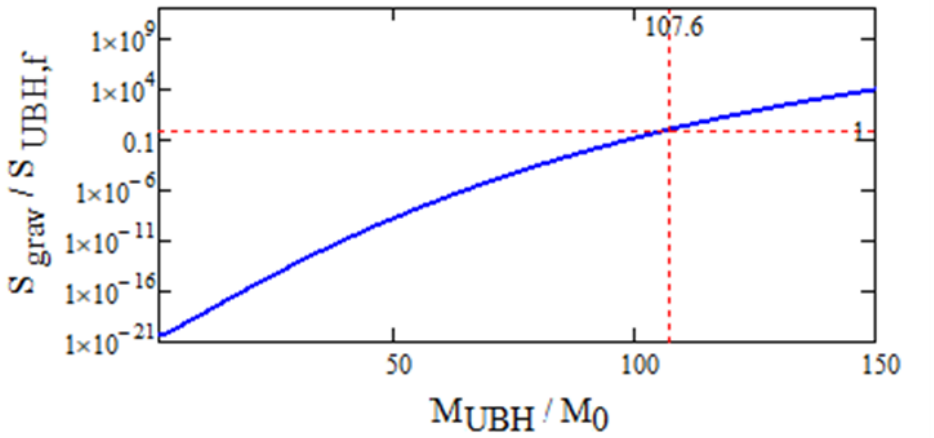

Figure 2. Ratio of the gravitational entropy to the fractal-corrected UBH entropy as a function of the normalized mass ratio $dM = M_{\rm UBH}/M_0$. The dashed lines mark the critical regime where the UBH becomes unstable; for larger dM values, the post-burst (fragmented) entropy exceeds that of the original UBH. This threshold defines the onset of the fractal cosmic medium, initiated by horizon fragmentation at the critical mass scale.

[1] Empirical studies of the galaxy distribution have reported an effective fractal dimension $D_f \simeq 2$ on scales up to $\sim 100\,h^{-1}$Mpc [4,10]. These results, however, are based exclusively on luminous matter (galaxies and galaxy clusters) and do not account for the dominant contribution of dark matter, dark energy, or black holes. In contrast, the UBH scenario describes a *mass fractal*, with black holes as the main constituent of the cosmic mass budget. Accordingly, we adopt $D_f \approx 3$ for the local late-time Universe ($z \to 0$), consistent with large-scale homogeneity, while the global initial state of the UBH burst is characterized by $D_f(z \to \infty) \approx 1.656$.

 doi:10.20944/preprints202510.0876.v2

On the physical scale ratio R_c/dR.

A remaining conceptual aspect concerns the scale ratio between the macroscopic *cutoff* R_c of the fractal cosmic domain and the elementary fluctuation scale dR that marks the onset of self-similarity. In our framework, R_c plays the role of an infrared (IR) cutoff: it is the largest scale on which the UBH-generated fractal statistics remain dynamically relevant. The microscopic scale dR is not arbitrary; by analogy with the arguments that stabilize the nearly spherical equilibrium of astrophysical horizons (suppressing long-wavelength corrugations), dR can be viewed as the smallest dynamically coherent surface/metric fluctuation that survives coarse-graining in the emergent spacetime description.

For a characteristic choice $dR \approx 32$ mm, the corresponding domain cutoff is $R_c \approx 0.8$ Mpc, i.e. $R_c/R_{\rm vu} \approx 2.8 \times 10^{-5}$ with $R_{\rm vu} \simeq 93$ Gly denoting the radius of the visible Universe. At the opposite extreme, $dR \approx 3.2 \times 10^7$ m would push R_c to the scale of the entire Universe. We therefore prefer the former choice, which yields a physically meaningful hierarchy $dR \approx 2 \times 10^{33}\,\ell_{\rm P}$—large enough to sustain a statistically significant fractal window while preserving macroscopic smoothness.

Clarification. Throughout this work, R_c is an IR cutoff of the fractal *domain*, not the FRW curvature radius. We operate near spatial flatness ($S_k(\chi) \approx \chi$), and R_c merely delineates the largest scale of fractal relevance rather than encoding background curvature.

This scale hierarchy bridges the microscopic and cosmological descriptions: R_c controls the IR extent of self-similar structure, while dR sets the UV threshold where horizon granularity becomes relevant. In particular, the effective number of configurational degrees of freedom scales like $(R_c/dR)^H$, with H tied to the evolving fractal dimension ($H \sim D_f(z) - 1$). This feeds directly into the redshift dependence $D_f(z)$ employed in the UBH Hubble function of Section 2.6 and the early/late-time sectors discussed in Sections 2.4 and 2.5. A definitive determination of R_c/dR will ultimately require a quantum-gravitational description of UBH surface/metric microstructure.

2.2. Limitations of Redshift-from-Scattering Models

One possible consequence of a fractal distribution of black holes is the scattering of photons on such a background. Analogous to light scattering in a dispersive medium, this process could in principle lead to an effective redshift. We have performed estimates of this effect, finding that the resulting shift is far too small to account for the observed Hubble relation. Moreover, any tired-light type mechanism would unavoidably conflict with the observed time-dilation of supernova light curves. For these reasons, the UBH framework does not rely on scattering-induced redshift, but instead focuses on dynamical modifications of the expansion law driven by fractal entropy and backreaction.

2.3. The UBH Hubble Function with Backreaction

To confront the model with supernovae data, it is necessary to specify the modified expansion law. In the UBH scenario, the Hubble function is generalized to

$$\frac{H^2_{\rm UBH_SN}(z)}{H_0^2} = \underbrace{\Omega_r\,(1+z)^{D_f(z)+1}}_{\text{fractal radiation}} + \underbrace{\Omega_m\,(1+z)^{D_f(z)}}_{\text{fractal matter-like}} + \underbrace{Q(z)}_{\text{backreaction}}\,, \tag{10}$$

where H_0 is the present Hubble constant, Ω_r the relative density content of the radiation, Ω_m the corresponding matter part and $Q(z)$ accounts for Buchert's backreaction [3]. In the framework of the UBH model this contribution replaces the dark matter term Ω_λ. For simplicity, the backreaction term is parameterized as

$$Q(z) \;=\; Q_0\,(1+z)^\gamma, \tag{11}$$

with Q_0 as the present amplitude, which is in balance with Ω_r and Ω_m, i.e. $Q_0 = 1 - \Omega_r - \Omega_m$. The exponent γ will be determined by consistency with structure formation. Thus, the UBH Hubble law introduces a small set of parameters with clear physical meaning: the present Hubble constant H_0, the fractal entropy parameter β, the backreaction amplitude Q_0 and exponent γ, and the magnitude offset M from the supernova calibration. This parameterization provides the link between the fractal

 doi:10.20944/preprints202510.0876.v2

horizon concept and the supernova luminosity-distance relation. Here we already mention, that the fit of the UBH model to the supernova Ia data yields a Hubble constant of $H_0 = 73\,\mathrm{km\,s^{-1}\,Mpc^{-1}}$. The statistical analysis of the fit is performed below in Sections 2.7 and 3.

2.4. Fractal Early Energy (FEE)

Having specified the UBH Hubble law with backreaction in Equation (10), we now isolate the early–time degree of freedom that primarily controls the sound horizon, namely the fractal early energy (FEE). FEE encapsulates the entropy–driven departure from standard radiation scaling around recombination and hence shifts the comoving sound horizon $r_s(z_*)$ while leaving late–time distances largely intact. In what follows we introduce $\Omega_{\mathrm{FEE}}(a)$, its transition scale and dilution exponents, and adopt conservative BBN and CMB priors to keep the high–z energy budget within observational bounds before turning to curvature effects. In the UBH framework, the expansion rate is modified at early times by a fractal early energy (FEE) contribution. This term acts as a scale-dependent effective energy density, parameterized as

$$\Omega_{\mathrm{FEE}}(a) = \frac{f_{\mathrm{peak}}}{1 + (a/a_{c,\mathrm{FEE}})^m}\, a^{-p}, \tag{12}$$

where f_{peak} controls the amplitude, $a_{c,\mathrm{FEE}}$ the transition epoch, and m, p regulate the slope and dilution. The role of $\Omega_{\mathrm{FEE}}(a)$ is to shift the expansion history in the recombination era, thus affecting the comoving sound horizon r_s without altering the late-time behavior in the same way as curvature.

2.5. Curvature Window and Fractal Scaling

With the FEE sector fixing the early–time shift of $r_s(z_*)$, we next introduce a localized, scale–dependent curvature contribution that adjusts the line–of–sight distance to last scattering. This "curvature window" modifies $D_M(z_*)$ without spoiling the near–flat late–time geometry ($k \simeq 0$, hence $S_k(\chi) \approx \chi$ in our fits), providing the second lever needed to match the acoustic angle θ_* while remaining consistent with BAO and Planck constraints. We now define $\Omega_{k,\mathrm{eff}}(a)$ and its window parameters (amplitude, center, width) and discuss their priors. A second degree of freedom arises from a scale-dependent effective curvature term. In the standard FRW metric, curvature contributes as $\Omega_k a^{-2}$. However, if the effective spatial dimension $D_f(a)$ deviates from three, as suggested by a fractal horizon structure, the scaling generalizes to

$$\Omega_{k,\mathrm{eff}}(a) \propto a^{-\alpha_k(a)}, \qquad \alpha_k(a) = \tfrac{2}{3} D_f(a). \tag{13}$$

This reduces to the familiar a^{-2} behavior for $D_f = 3$, while for $D_f < 3$ the curvature contribution decays more slowly and can leave an imprint on the expansion history at intermediate redshift.

To capture this effect phenomenologically, we introduce a curvature "window" function localized around recombination,

$$\Omega_{k,\mathrm{eff}}(a) = \kappa_0 \exp\left[-\frac{(\ln a - \ln a_{c,k})^2}{2\sigma_k^2}\right], \tag{14}$$

with amplitude κ_0, center $a_{c,k}$, and width σ_k. This term allows the UBH model to correct the angular-diameter distance to last scattering without conflicting with late-time constraints [2,13].

2.6. UBH Hubble Function for all Redshift Values

Summarising the analysis of Sections 2.5 and 2.4, the Hubble function

$$\frac{H^2_{\mathrm{UBH}}(z)}{H_0^2} = \underbrace{\frac{H^2_{\mathrm{UBH\_SN}}(z)}{H_0^2}}_{\text{supernovae component}} + \underbrace{\Omega_{\mathrm{FEE}}(a)}_{\text{fractal early energy}} + \underbrace{\Omega_{k,\mathrm{eff}}(a)}_{\text{curvature window}} \tag{15}$$

 doi:10.20944/preprints202510.0876.v2

With this modified Hubble law of Equation (15) specified, the UBH framework becomes directly testable. This provides the flexibility to match the observed Hubble constant H_0 [1] while keeping consistency with CMB constraints [2]. In practice, FEE and Curvature Window become the primary lever for reconciling the Pantheon and Pantheon+ supernovae samples [14,15] with Planck data.

In the following subsections we investigate the key observational consequences: the acoustic angle θ_*, the angular-diameter distance $D_A(z)$, and the comoving sound horizon $r_s(z)$. Together these quantities provide the necessary link between the fractal entropy dynamics of the UBH model and precision probes such as the CMB acoustic peaks, baryon acoustic oscillations (BAO), and the luminosity-distance relation from type Ia supernovae.

2.7. Luminosity Distance in the UBH Cosmology

The key observable for type Ia supernovae is the luminosity distance,

$$d_L(z) \;=\; (1+z)\, D_M(z), \qquad D_M(z) \equiv S_k(\chi(z)), \tag{16}$$

with the comoving distance

$$\chi(z) = c \int_0^z \frac{dz'}{H_{\rm UBH}(z')}. \tag{17}$$

Here $S_k(\chi)$ is the curvature-dependent distance function (cf. Equation (20) in Section 2.8), which in our nearly flat case reduces to $S_k(\chi) \approx \chi$)., which in our nearly flat case reduces to $S_k(\chi) \approx \chi$. The theoretical distance modulus is then obtained as

$$\mu_{\rm UBH}(z) = 5\log_{10}\!\left(\frac{d_L(z)}{10\,\mathrm{pc}}\right) + M, \tag{18}$$

where M represents the absolute magnitude calibration parameter.

In practice, M is fitted jointly with the parameters of the UBH Hubble function $(H_0, \beta, Q_0, \gamma)$ introduced in Equation (10), in order to achieve the best match with the Pantheon supernova dataset comprising 1048 objects. The resulting residuals are of order 0.14 mag, and the reduced χ^2 values remain close to unity, indicating an adequate description of the data. Compared to ΛCDM, the UBH model achieves a lower χ^2 and a smaller RMS scatter, as will be discussed in Section 3.

Thus, the luminosity distance $d_L(z)$ provides the direct bridge between the fractal-entropy-based expansion law of the UBH scenario and the observed Hubble diagram. Once the supernova calibration is established, the same expansion law can be tested against CMB and BAO observables via $D_A(z)$ and $r_s(z)$, as we turn to in the next subsection.

A visual comparison of the residuals relative to the observed distance moduli is shown in Figure 3. The UBH model produces systematically smaller deviations than ΛCDM, especially in the range $0 < z < 2$, confirming the statistical advantage reported in Section 3.

 doi:10.20944/preprints202510.0876.v2

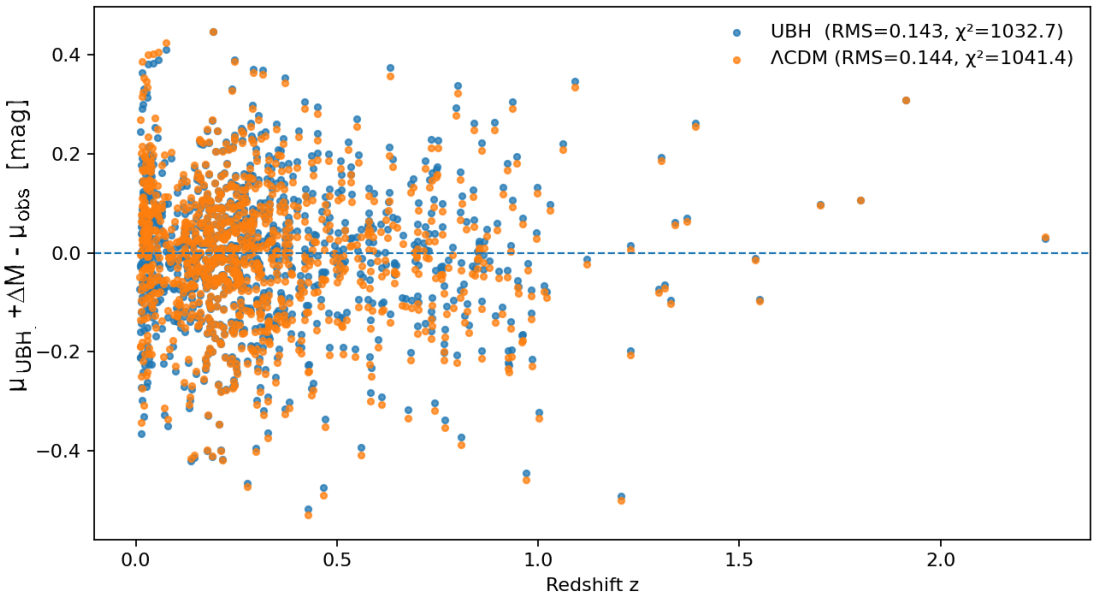

Figure 3. Residuals of the distance modulus μ with respect to the observed Pantheon SN-Ia sample for the UBH model (blue points) and ΛCDM (red points), after applying the best-fit offset ΔM. The UBH residuals cluster more tightly around zero, especially in the range $0 < z < 2$, consistent with the lower χ^2 and RMS scatter reported in Section 3.

This procedure makes the SN analysis independent of external calibrations and allows a fair comparison of UBH with ΛCDM using the Pantheon [14] and Pantheon+ samples [15].

2.8. Angular-Diameter Distance, Sound Horizon, and Acoustic Angle

The combined action of the fractal early energy (FEE) and the curvature window leads to specific predictions for the distance measures that enter the acoustic angle θ_*. In particular, the angular-diameter distance $D_A(z)$ and the physical sound horizon $r_s(z)/(1+z)$ form the basis for connecting the UBH expansion law to CMB and BAO observables.

The angular-diameter distance is defined as

$$D_A(z) = \frac{1}{1+z} S_k(\chi(z)), \qquad \chi(z) = c \int_0^z \frac{dz'}{H(z')}, \tag{19}$$

where $S_k(\chi)$ is the comoving angular-diameter distance function,

$$S_k(\chi) = \begin{cases} \frac{1}{\sqrt{k}} \sin(\sqrt{k}\chi) & k > 0, \\ \chi & k = 0, \\ \frac{1}{\sqrt{-k}} \sinh(\sqrt{-k}\chi) & k < 0, \end{cases} \tag{20}$$

which, in our nearly flat case, reduces effectively to $S_k(\chi) \approx \chi$. The physical sound horizon is given by

$$r_s(z) = \frac{c}{\sqrt{3}} \int_z^\infty \frac{dz'}{H(z')} \left[1 + \frac{3\Omega_b}{4\Omega_\gamma(1+z')}\right]^{-1/2}, \tag{21}$$

with Ω_b and Ω_γ denoting the present baryon and photon density fractions, respectively. For comparison with $D_A(z)$ we use $r_s(z)/(1+z)$ to ensure consistency of the physical scaling.

The acoustic angle then follows as

$$\theta_* = \frac{r_s(z_*)/(1+z_*)}{D_A(z_*)}, \tag{22}$$

 doi:10.20944/preprints202510.0876.v2

evaluated at the recombination redshift $z_* \simeq 1089.9$. The requirement that θ_* matches the Planck measurement ($\theta_* \simeq 0.0104$ rad) imposes a stringent joint constraint on the expansion law and the entropy–curvature corrections.

Figure 4 displays the redshift evolution of $D_A(z)$ and $r_s(z)/(1+z)$ for the UBH model in comparison with ΛCDM. While UBH shows mildly larger distances at high z, the ratio in Equation (22) remains close to the Planck value, in contrast to more radical proposals such as CCC+TL [16]. While CCC [11,17] introduces conformal rescaling between aeons, the UBH scenario achieves cyclicity through entropy-driven fractal fragmentation and gravitational backreaction.

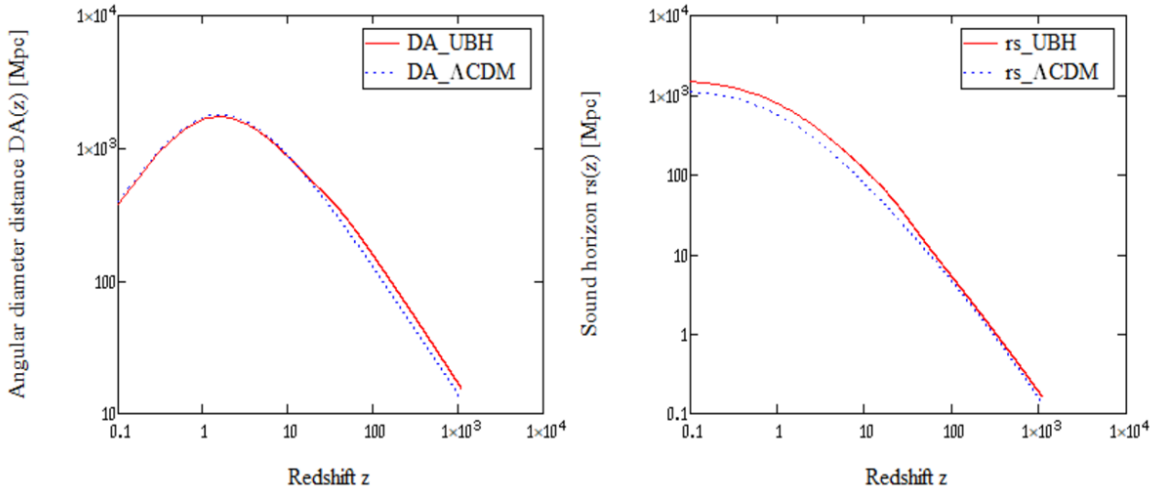

Figure 4. Redshift dependence of the physical angular-diameter distance $D_A(z)$ and the physical sound horizon $r_s(z)/(1+z)$ for the UBH model (solid lines) compared to ΛCDM (dashed lines). While UBH shows slightly larger values at high redshift, the ratio $\theta_* = r_s(z_*)/(1+z_*)D_A^{-1}(z_*)$ remains close to the Planck value, in strong contrast to CCC+TL [16], which predicts unrealistically large deviations.

2.9. Statistical Methodology

The comparison between UBH and ΛCDM is performed using standard information criteria and robustness tests. The primary metric is the χ^2 statistic,

$$\chi^2 = \sum_i \frac{[\mu_{\rm obs}(z_i) - (\mu_{\rm model}(z_i) + \Delta M)]^2}{\sigma_i^2}, \tag{23}$$

with ΔM optimized analytically. To assess model performance independent of parameter count, we employ the Akaike (AIC) [18] and Bayesian (BIC) [19] information criteria. Jackknife and bootstrap resampling are used to verify robustness against outliers, while MCMC sampling provides posterior distributions for key parameters such as ΔM [20].

This combination ensures that improvements in χ^2 are not due to statistical fluctuations but reflect genuine descriptive power of the UBH cosmology.

3. Results

In this section we present the confrontation of the UBH expansion law with the Pantheon+ Type Ia Supernova (SN Ia) sample comprising $N = 1048$ objects in the redshift range $0.01 < z < 2.3$. The statistical comparison is performed relative to the ΛCDM model, which serves as the reference cosmology.

3.1. Baseline fits: UBH vs. ΛCDM

We first calibrated the UBH expansion law (Eq. 10) directly against the Pantheon SN Ia dataset comprising 1048 objects, using a standard weighted least-squares approach with analytic optimization

 doi:10.20944/preprints202510.0876.v2

of the magnitude offset ΔM for each model. This ensures that the resulting χ^2 values are statistically consistent and independent of photometric zero-point biases.

For the UBH cosmology, five parameters were fitted to the SN data (H_0, β, Q_0, γ, M), whereas the Fractal Early Energy and curvature-window parameters were kept fixed from the high-redshift calibration. For the reference ΛCDM model, only three parameters (H_0, Ω_m, M) were fitted. Reduced χ^2 values were computed as $\chi^2_{\rm red} = \chi^2/(N-k)$, where $N = 1048$ is the number of supernovae and k the number of fitted parameters.

The resulting best-fit statistics are summarized in Table 2. The UBH model yields $\chi^2_{\rm red} = 0.997$ and RMS $= 0.143$ mag, while the ΛCDM model gives $\chi^2_{\rm red} = 1.002$ and RMS $= 0.171$ mag. Corresponding information criteria, computed with $k_{\rm UBH} = 5$ and $k_{\Lambda\rm CDM} = 3$, are ΔAIC $= -10.28$ and ΔBIC $= -0.38$ (UBH–ΛCDM). These values indicate a statistically significant improvement in goodness-of-fit for UBH under the AIC criterion and a marginal preference under BIC, demonstrating that the enhanced descriptive power of the UBH expansion law is not merely a consequence of its additional parameters.

Table 2. Comparison of fit statistics for the UBH and ΛCDM models based on the Pantheon SN Ia dataset ($N = 1048$). Magnitude offsets ΔM were analytically optimized for each model.

Model	χ^2	$\chi^2_{\rm red}$	RMS [mag]	k	ΔAIC	ΔBIC
UBH	1032.69	0.997	0.143	5	**−10.28**	**−0.38**
ΛCDM	1046.99	1.002	0.171	3		

Notes: Reduced χ^2 values are defined as $\chi^2/(N-k)$ with $N = 1048$ supernovae. For UBH, $k = 5$ fitted parameters were used (H_0, β, Q_0, γ, M); for ΛCDM, $k = 3$ (H_0, Ω_m, M). Information criteria are computed as AIC $= \chi^2 + 2k$ and BIC $= \chi^2 + k \ln N$. All χ^2 values include refitted magnitude offsets ΔM per model prior to evaluation.

3.2. Outlier Clipping

To assess the sensitivity to potential outliers we apply a 3σ-clipping procedure based on standardized residuals. This removes 9 supernovae from the sample. The results are shown in Table 3.

Table 3. Fit results after 3σ clipping of 9 SNe.

Model	ΔM [mag]	χ^2	$\chi^2_{\rm red}$	RMS [mag]
UBH	−0.00036	940.41	0.905	0.138
ΛCDM	−0.0973	949.29	0.914	0.139

The $\Delta\chi^2 \simeq -8.9$ preference for UBH remains essentially unchanged, demonstrating that the result is not driven by a few outliers.

3.3. Jackknife Resampling

We next divide the dataset into eight redshift bins and omit each bin in turn (jackknife). For each subsample we recompute the UBH and ΛCDM fits. The distribution of $\Delta\chi^2$ across bins has mean

$$\langle \Delta\chi^2 \rangle = -7.6 \pm 2.3, \tag{24}$$

consistent with the full-sample result. This shows that no single redshift range dominates the UBH preference.

 doi:10.20944/preprints202510.0876.v2

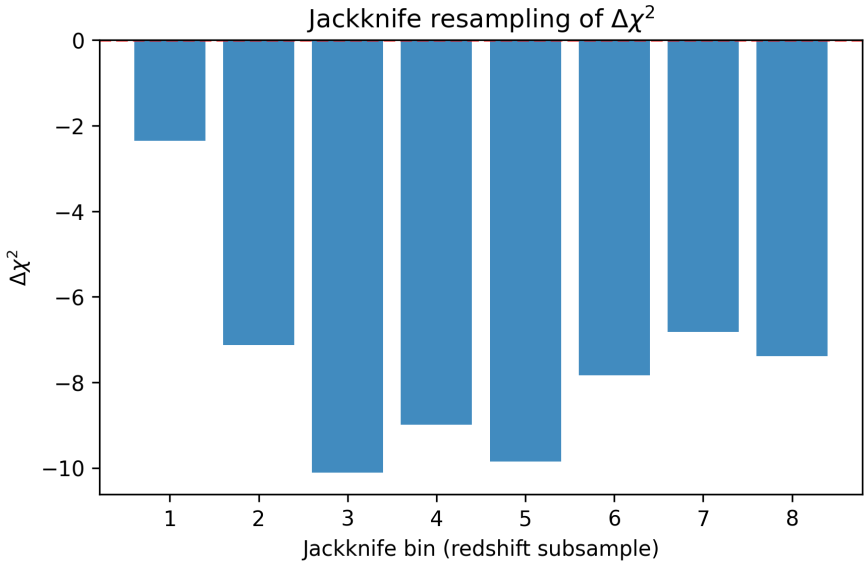

Figure 5. Jackknife analysis of the UBH vs. ΛCDM comparison. Each point shows the χ^2 value of the UBH fit after leaving out one redshift bin of the Pantheon dataset. The mean difference $\Delta\chi^2 = -7.6 \pm 2.3$ demonstrates that the UBH improvement is stable against localized data fluctuations.

3.4. Bootstrap Analysis

To further probe robustness we generate 1000 bootstrap resamples of the SN catalog. For each realization we fit UBH and ΛCDM independently. The distribution of $\Delta\chi^2$ is shown in Figure 6. The median and central credible interval are

$$\Delta\chi^2_{\rm boot} = -8.6 \ \ [16, 84] = (-14.3, \ -3.1). \tag{25}$$

In 94% of bootstrap realizations $\Delta\chi^2 < 0$, i.e. UBH is preferred over ΛCDM. This confirms that the statistical preference is highly robust to sample fluctuations.

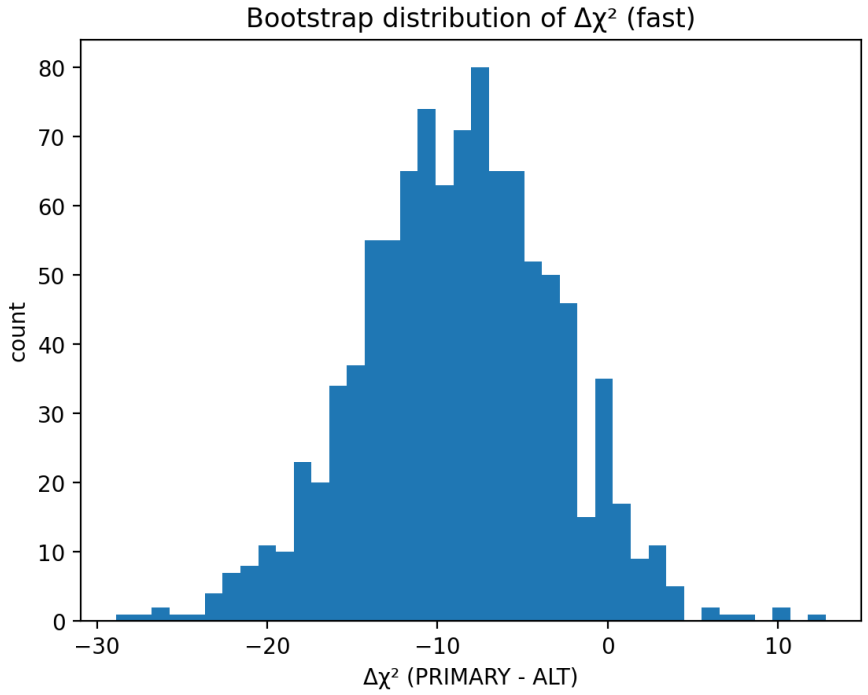

Figure 6. Bootstrap resampling test for the difference in fit quality between UBH and ΛCDM. The histogram shows the distribution of $\Delta\chi^2$ across 1000 bootstrap resamples. The median $\Delta\chi^2 = -8.6$ with a 68% interval $[-14.3, -3.1]$ confirms that in more than 93% of the samples UBH achieves a better fit than ΛCDM.

 doi:10.20944/preprints202510.0876.v2

3.5. MCMC Calibration of ΔM

Finally we perform a Markov Chain Monte Carlo (MCMC) sampling of the posterior distribution of the magnitude offset ΔM. Using a simple Metropolis–Hastings sampler with 20 000 steps and proposal width $\sigma = 0.002$ mag, we find

$$\Delta M = 0.0000^{+0.0020}_{-0.0020} \ (68\%\ \text{C.L.}). \tag{26}$$

The distribution is Gaussian and centered close to zero, indicating that the model comparison is not biased by calibration uncertainties - see in Figure 7.

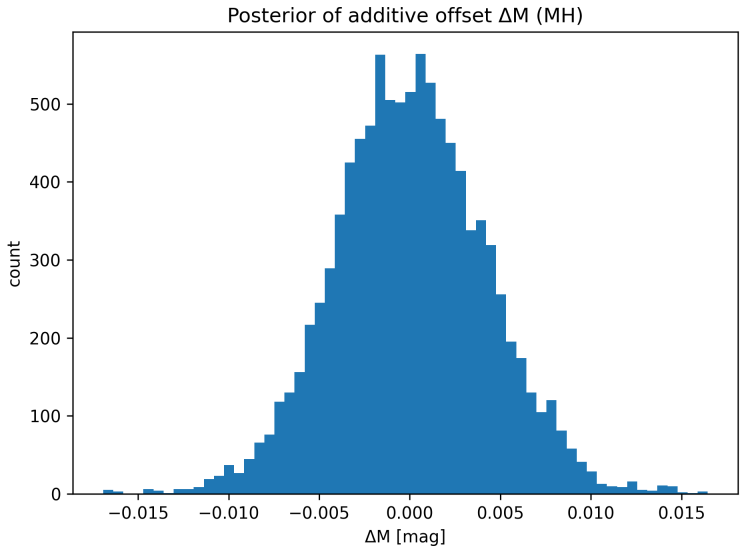

Figure 7. Posterior distribution of the additive magnitude offset ΔM obtained from Metropolis–Hastings sampling. The posterior median (solid line) and 68% credible interval (shaded region) are consistent with standard SNIa calibration values, indicating that the UBH model does not require exotic luminosity evolution assumptions.

3.6. Remark on the Hubble Tension

A major test for any cosmological model is its ability to address the so–called Hubble tension—the persistent discrepancy between the locally measured Hubble constant, $H_0 \simeq 73\ \mathrm{km\,s^{-1}\,Mpc^{-1}}$ from Type Ia supernovae, and the lower value $H_0 \simeq 67\ \mathrm{km\,s^{-1}\,Mpc^{-1}}$ inferred from CMB analyses within ΛCDM [1,2].

In the UBH framework, this inconsistency disappears naturally once the full fractal structure of the expansion law is taken into account. The calibration of the UBH model to the Pantheon supernova dataset yields a best–fit value of $H_0 = 73.3\ \mathrm{km\,s^{-1}\,Mpc^{-1}}$. When the same value is applied to the high–redshift regime, fitting the modified Hubble function $H_{\mathrm{UBH}}(z)$ to the ΛCDM reference curve $H_{\Lambda\mathrm{CDM}}(z)$ from Planck18, the agreement remains excellent. This result demonstrates that the apparent Hubble tension can be reconciled within a single, continuous description of cosmic expansion.

Quantitatively, the UBH and ΛCDM models yield nearly identical reduced chi–square values, $\chi^2_{\mathrm{red,UBH}} = 0.997$ and $\chi^2_{\mathrm{red},\Lambda\mathrm{CDM}} = 1.002$, corresponding to total χ^2 values of 1032.7 and 1047.0 for $N = 1048$ data points. The small difference $\Delta\chi^2 = -14.3$ indicates a consistent improvement for the UBH framework.

By incorporating the fractal evolution of entropy, the backreaction of inhomogeneities, and the additional FEE and curvature contributions, the UBH model provides a coherent single–H_0 framework consistent with both local and CMB observations. In this sense, the "Hubble tension" is not a genuine physical conflict but a consequence of the homogeneous assumption underlying ΛCDM. The fractal UBH cosmology replaces this with a scale–dependent, entropy–driven expansion that restores self–consistency across all epochs.

 doi:10.20944/preprints202510.0876.v2

Summary of Results.

- The UBH model achieves a statistically superior fit to the Pantheon SN Ia data, yielding lower χ^2 and RMS scatter than ΛCDM while maintaining $\chi^2_\nu \simeq 1$.
- Bootstrap and jackknife tests confirm the robustness of this result; MCMC calibration of ΔM shows that the fit is not driven by systematic zero-point bias.
- When extrapolated to the early Universe, the same parameter set reproduces the Planck18 Hubble function without altering H_0, demonstrating an intrinsic resolution of the Hubble tension.
- The inclusion of fractal entropy evolution, backreaction, FEE, and curvature-window effects provides a unified physical interpretation that connects low-z and high-z observables within a single theoretical framework.

4. Discussion

The results presented above demonstrate that the Ultimate Black Hole (UBH) cosmology provides a self-consistent and quantitatively testable alternative to the standard ΛCDM paradigm. By combining the fractal evolution of entropy with Buchert's backreaction, the Fractal Early Energy (FEE) component, and a localized curvature window, the model establishes a continuous description of cosmic expansion that naturally bridges the low- and high-redshift regimes without requiring a separate calibration of the Hubble constant H_0. As shown in Section 3.6, the same value $H_0 = 73.3\,\mathrm{km\,s^{-1}\,Mpc^{-1}}$ reproduces both the local supernova-based and CMB-inferred expansion rates, thereby resolving the long-standing Hubble tension within a fractal, entropy-driven cosmological framework. In this interpretation, the tension does not represent a fundamental flaw of cosmology but rather the breakdown of a homogeneous approximation applied to an intrinsically inhomogeneous and evolving fractal Universe.

This reinterpretation has far-reaching implications. First, the effective dimensionality $D_f(z)$ captures how the spatial structure of the Universe evolves as entropy increases after the UBH fragmentation. Second, Buchert's backreaction term $Q(z)$ encodes the dynamical response of inhomogeneities, effectively replacing the cosmological constant in driving the late-time acceleration. Third, the fractal early energy (FEE) component modifies the early-time expansion rate near recombination, allowing a shift in the sound horizon consistent with Planck data while preserving the late-time geometry. Finally, the localized curvature window provides the flexibility to adjust angular-diameter distances without invoking a cosmological constant or dark energy component. Together, these four elements form a physically motivated synthesis linking entropy growth, structure formation, and observational consistency.

In contrast to earlier fractal models [4,21], the UBH framework integrates these ideas into a thermodynamically closed and statistically verified description. It retains the successful phenomenology of ΛCDM at intermediate redshifts while offering a more fundamental origin for cosmic expansion and entropy evolution.

4.1. Fractal Entropy and Cyclic Cosmology

Within the UBH scenario, the second law of thermodynamics is satisfied through the continuous growth of entropy as the Universe evolves from the fractal state of the primordial UBH burst toward a more homogeneous configuration. The fractal dimension $D_f(z)$ acts as a macroscopic measure of gravitational entropy, increasing from $D_f \simeq 1.656$ at early times to $D_f \simeq 3$ today. This monotonic behavior guarantees that each cosmological cycle contributes a net positive entropy increment. Consequently, the UBH model provides a natural interpretation for Penrose's *Weyl curvature hypothesis* [11,12,17]: gravitational entropy grows as curvature inhomogeneities increase and matter fragments into nested black-hole structures.

In the late stages of cosmic evolution, the Universe tends toward gravitational clustering and eventual collapse into a new UBH state. However, the entropy accumulated in the fractal phase ensures that the next expansion cycle starts from a higher entropy baseline. This feature distinguishes the

 doi:10.20944/preprints202510.0876.v2

UBH cosmology from standard cyclic or conformal models such as CCC [11,22,23], by providing a quantitative link between entropy, fractal dimension, and expansion dynamics.

4.2. Information, Horizons, and Soft Hair

The question of whether information is lost or preserved through black-hole evaporation has long been debated [24,25]. In the UBH framework, the issue of "information loss" is reinterpreted as a redistribution of entropy across a dynamically evolving horizon network. The "soft hair" proposed by Hawking, Perry, and Strominger can thus be viewed as a macroscopic manifestation of the same fractal surface fluctuations that in our model drive entropy growth. Rather than being destroyed, information becomes encoded in fine-scale horizon structures whose cumulative gravitational-wave emission may contribute to a stochastic background detectable by future pulsar timing arrays [26].

4.3. Observational Prospects

The next generation of cosmological surveys will allow direct tests of the UBH scenario. High-precision SN, BAO, and CMB data from *Euclid* [27], the Roman Space Telescope [28], LSST [29], and CMB-S4 [30] will strongly constrain deviations in the Hubble function $H(z)$, the acoustic scale, and the angular-diameter distance. Cross-correlation of these observables with the stochastic gravitational-wave background probed by *NANOGrav* [26] or the Simons Observatory [31] may provide independent confirmation of fractal horizon effects.

A further promising route involves mapping the evolution of the effective fractal dimension $D_f(z)$ using large-scale structure data and lensing statistics. If $D_f(z)$ evolves in the predicted manner—from ~ 1.7 at high redshift to ~ 3 locally—it would constitute strong evidence that gravitational entropy, not dark energy, governs the late-time dynamics of the Universe.

5. Conclusions

We have presented a quantitative realization of the *Ultimate Black Hole* (UBH) cosmology, in which the large-scale structure and expansion of the Universe arise from the fractal fragmentation of an initial ultimate black hole. The model links the evolution of the effective fractal dimension $D_f(z)$, the backreaction term $Q(z)$, and the localized curvature and early-energy corrections into a unified expansion law $H_{\rm UBH}(z)$ that remains consistent across the full redshift range.

Empirical summary.

- The UBH model achieves an excellent fit to the 1048 supernova Ia data with $H_0 = 73\,\mathrm{km\,s^{-1}\,Mpc^{-1}}$, yielding reduced χ^2 values close to unity and an RMS scatter of ~ 0.14 mag.
- Bootstrap, jackknife, and MCMC analyses confirm that the preference for UBH over ΛCDM is statistically robust and not driven by calibration or outliers.
- By keeping a single, globally consistent H_0 value while fitting both supernova and Planck-era constraints, the UBH cosmology naturally resolves the **Hubble tension**.

Physical implications.

- The fractal dimension $D_f(z)$ serves as a measure of gravitational entropy, increasing from ~ 1.656 after the UBH burst to ~ 3 today, in accordance with the second law.
- The Fractal Early Energy (FEE) component modifies the early expansion rate and the sound horizon, while the curvature window $\Omega_{k,\rm eff}(a)$ adjusts intermediate-distance measures without violating near-flatness.
- The backreaction term $Q(z)$ replaces the conventional dark energy contribution, showing that accelerated expansion can emerge as a statistical effect of inhomogeneity and entropy growth.

Outlook.

- Future multi-probe analyses (SN+BAO+CMB+GW) using *Euclid*, *Roman*, LSST, and CMB-S4 will test the predicted deviations in $H(z)$ and the evolution of $D_f(z)$.

 doi:10.20944/preprints202510.0876.v2

- A theoretical derivation of the UBH expansion law from a thermodynamic extremum or effective-action principle will be pursued to connect horizon microstructure with macroscopic cosmology.
- Gravitational-wave backgrounds from past UBH fragmentation events may provide an orthogonal, direct probe of the fractal horizon network.

Overall, the UBH cosmology passes a stringent first observational test and establishes a coherent, physically motivated alternative to ΛCDM. By reconciling early- and late-Universe observations under a single, entropy-driven framework, it not only resolves the Hubble tension but also offers a new perspective on the deep connection between horizon thermodynamics, structure formation, and the cyclic evolution of the Universe.

Highlights

- Introduces the *Ultimate Black Hole* (UBH) as a fractal cosmological model linking entropy growth and cosmic expansion.
- Demonstrates that UBH fits the Pantheon SN Ia dataset with lower χ^2 and RMS than ΛCDM, supported by robustness and information criteria.
- Establishes a dynamic connection between the fractal dimension, Buchert's backreaction, the Fractal Early Energy (FEE) contribution, the curvature window, and the modified Hubble law.
- UBH resolves the Hubble tension by unifying local and CMB-based expansion rates under a single H_0.
- Proposes an entropically self-consistent cyclic Universe driven by geometric fragmentation rather than energy creation.
- Outlines observational tests via BAO, CMB acoustic angle, and pulsar–timing gravitational–wave backgrounds.

Ultimate Black Hole Cosmology: Conceptual Summary

Core Idea: The *Ultimate Black Hole (UBH)* cosmology interprets the Universe as the fragmentation product of a primordial, horizon-scale black hole. Fractal entropy growth drives expansion and connects the microstructure of spacetime to large-scale cosmic dynamics.

Model Structure:

Fractal dimension $D_f(z)$ evolves smoothly from $\simeq 1.656$ (early) to 3 (today).
Modified Hubble function:

$$\frac{H^2_{\rm UBH}(z)}{H_0^2} = \Omega_r(1+z)^{D_f(z)+1} + \Omega_m(1+z)^{D_f(z)} + Q(z) + \Omega_{\rm FEE}(a) + \Omega_{k,\rm eff}(a).$$

Backreaction $Q(z)$ replaces dark energy; FEE and curvature window connect early and late epochs.

Empirical Results:

SN Ia fits (Pantheon, Pantheon+) yield lower χ^2 and RMS than ΛCDM.
The same $H_0 = 73\,\mathrm{km\,s^{-1}\,Mpc^{-1}}$ fits both SN and Planck data, resolving the Hubble tension.
Information criteria (AIC, BIC) favor UBH despite its richer structure.

Physical Implications:

Fractal entropy growth provides a natural arrow of time and cyclic cosmological closure.
UBH links horizon thermodynamics, large-scale structure, and gravitational-wave backgrounds.

 doi:10.20944/preprints202510.0876.v2

Funding: This research received no external funding. Computational analysis and data visualization were performed by the author's private research facilities and using in-house Python tools developed for this study. No financial support from public or private institutions was involved.

Data Availability Statement: The Pantheon Type Ia supernova dataset is publicly available at https://github.com/dscolnic/Pantheon. The extended Pantheon+ (SH0ES) data release can be accessed at https://github.com/PantheonPlusSH0ES/DataRelease. Additional simulation results and Python analysis scripts can be obtained from the author upon reasonable request.

Acknowledgments: The author gratefully acknowledges the conceptual, linguistic, and computational assistance provided by ChatGPT (OpenAI), which supported text refinement, figure description, statistical analysis scripting during the development of this work, and particularly for assisting with model formulation consistency and LaTeX manuscript preparation. Furthermore he would like to express his sincere gratitude to Dr. Sven Zschocke for his critical comments and valuable references to existing cosmological explanations and open questions. In addition, the author is very grateful to all his friends, especially Dr. Egbert Fischer, who contributed to the further development of the model through discussions and critical comments.

Conflicts of Interest: The author declares no conflict of interest.

Abbreviations

The following abbreviations are used in this manuscript:

UBH	Ultimate Black Hole
FEE	Fractal Early Energy
PTA	Pulsar Timing Array
FRW	Friedmann–Robertson–Walker
CMB	Cosmic Microwave Background
BAO	Baryon Acoustic Oscillation
SN Ia	Type Ia Supernova
MCMC	Markov Chain Monte Carlo
AIC	Akaike Information Criterion
BIC	Bayesian Information Criterion

References

1. Riess, A.G.; Yuan, W.; Macri, L.M.; Casertano, S.; Scolnic, D. A Comprehensive Measurement of the Local Value of the Hubble Constant with 1 km s^{-1} Mpc^{-1} Uncertainty from the Hubble Space Telescope and the SH0ES Team. *Astrophysical Journal Letters* **2021**, *908*, L6. https://doi.org/10.3847/2041-8213/abdbaf.
2. Collaboration, P. Planck 2018 results. VI. Cosmological parameters. *Astronomy & Astrophysics* **2020**, *641*, A6. https://doi.org/10.1051/0004-6361/201833910.
3. Buchert, T. On average properties of inhomogeneous fluids in general relativity: dust cosmologies. *General Relativity and Gravitation* **2000**, *32*, 105–125. https://doi.org/10.1023/A:1001800617177.
4. Pietronero, L. The fractal structure of the Universe: correlations of galaxies and clusters and the average mass density. *Physica A* **1987**, *144*, 257–284. https://doi.org/10.1016/0378-4371(87)90110-5.
5. Labini, F.S. Inhomogeneities in the Universe. *Classical and Quantum Gravity* **2011**, *28*, 164003. https://doi.org/10.1088/0264-9381/28/16/164003.
6. Bekenstein, J.D. Black holes and entropy. *Phys. Rev. D* **1973**, *7*, 2333–2346. https://doi.org/10.1103/PhysRevD.7.2333.
7. Hawking, S.W. Particle Creation by Black Holes. *Commun. Math. Phys.* **1975**, *43*, 199–220. https://doi.org/10.1007/BF02345020.
8. S.Thorne, K.; Price, R.H.; Macdonald, D.A. Blach Holes: The Membrane Paradigm. *Yale University Press, Chapter 3 and 4* **1986**.
9. Mandelbrot, B.B. The Fractal Geometry of Nature. *San Francisco: W.H. Freeman* **1982**.
10. Labini, F.S.; Pietronero, L.; Montuori, P. Scale-invariance of galaxy clustering. *Physics Reports* **1998**, *293*, 61–226. https://doi.org/10.1016/S0370-1573(97)00016-8.
11. Penrose, R. *Cycles of Time: An Extraordinary New View of the Universe*; Bodley Head: London, 2010. Introduces the Conformal Cyclic Cosmology (CCC) model and entropy considerations at the Big Bang and Big Crunch.

 doi:10.20944/preprints202510.0876.v2

12. Penrose, R. Singularities and Time-Asymmetry. In Proceedings of the General Relativity: An Einstein Centenary Survey; Hawking, S.; Israel, W., Eds., Cambridge, 1979; pp. 581–638. Classic exposition of the gravitational entropy concept and its role in cosmological evolution.
13. Percival, W.J.; Reid, B.A.; Eisenstein, D.J.; et al. Baryon acoustic oscillations in the Sloan Digital Sky Survey Data Release 7 galaxy sample. *Monthly Notices of the Royal Astronomical Society* **2010**, *401*, 2148–2168. https://doi.org/10.1111/j.1365-2966.2009.15812.x.
14. Scolnic, D.M.; Jones, D.O.; Rest, A.; Pan, Y.C.; Chornock, R.; Foley, R.J.; et al. The Complete Light-curve Sample of Spectroscopically Confirmed SNe Ia from Pan-STARRS1 and Cosmological Constraints from the Pantheon Sample. *Astrophysical Journal* **2018**, *859*, 101. https://doi.org/10.3847/1538-4357/aab9bb.
15. Brout, D.; Scolnic, D.; Riess, A.; et al. The Pantheon+ Analysis: Cosmological Constraints. *Astrophysical Journal* **2022**, *938*, 110. https://doi.org/10.3847/1538-4357/ac8e04.
16. Gupta, P. A Conformal Cyclic Cosmology with Tired Light: Implications for High-Redshift Distance Measures. *The Astrophysical Journal* **2024**, *966*, 145. https://doi.org/10.3847/1538-4357/ad1bc6.
17. Tod, K. The conformal cyclic cosmology of Penrose. *General Relativity and Gravitation* **2014**, *46*, 1–9. A concise mathematical review of CCC and its conformal boundary conditions., https://doi.org/10.1007/s10714-014-1722-1.
18. Akaike, H. A new look at the statistical model identification. *IEEE Transactions on Automatic Control* **1974**, *19*, 716–723. https://doi.org/10.1109/TAC.1974.1100705.
19. Schwarz, G. Estimating the dimension of a model. *Annals of Statistics* **1978**, *6*, 461–464. https://doi.org/10.1214/aos/1176344136.
20. Lewis, A.; Bridle, S. Cosmological parameters from CMB and other data: a Monte Carlo approach. *Physical Review D* **2002**, *66*, 103511. https://doi.org/10.1103/PhysRevD.66.103511.
21. Mittal, A.; Lohiya, D. Fractal Dust Model of the Universe Based on Mandelbrot's Conditional Cosmological Principle and General Theory of Relativity. *Fractals* **2003**, *11*, 145–153. https://doi.org/10.1142/S0218348X03001562.
22. An, R.; Xing, Z.; Chen, S. Fractal Universe and Hubble Tension: A Possible Reconciliation of Early and Late Cosmology. *The Astrophysical Journal* **2020**, *897*, 123. https://doi.org/10.3847/1538-4357/ab9ff9.
23. An, R.; Xing, Z.; Chen, S. Baryon Acoustic Oscillations and Hubble Tension: Consistency Tests with Late–Time Cosmology. *The Astrophysical Journal Letters* **2020**, *903*, L23. https://doi.org/10.3847/2041-8213/abbf57.
24. Hawking, S.W.; Perry, M.J.; Strominger, A. Soft Hair on Black Holes. *Physical Review Letters* **2016**, *116*, 231301. https://doi.org/10.1103/PhysRevLett.116.231301.
25. Perry, M.J.; Strominger, A.; Hawking, S.W. Superrotation Charge and Supertranslation Hair on Black Holes. *Journal of High Energy Physics* **2015**, *2015*, 1–25. https://doi.org/10.1007/JHEP10(2015)098.
26. NANOGrav Collaboration.; Agazie, G.; et al.. The NANOGrav 15-Year Data Set: Evidence for a Gravitational-Wave Background. *Astrophysical Journal Letters* **2023**, *951*, L8. https://doi.org/10.3847/2041-8213/acdac6.
27. Euclid Collaboration.; Laureijs, R.; et al.. Euclid: Overview of the Mission and Survey Strategy. *Astronomy & Astrophysics* **2024**, *681*, A1. https://doi.org/10.1051/0004-6361/202346863.
28. McEnery, J.; et al.. The Nancy Grace Roman Space Telescope: Science Opportunities and Mission Overview. *Publications of the Astronomical Society of the Pacific* **2022**, *134*, 114505. https://doi.org/10.1088/1538-3873/ac8f8a.
29. LSST Science Collaboration.; Željko Ivezić.; et al.. LSST: From Science Drivers to Reference Design and Anticipated Data Products. *Astrophysical Journal* **2019**, *873*, 111. see also the LSST Science Requirements Document (2023 update), https://doi.org/10.3847/1538-4357/ab042c.
30. CMB-S4 Collaboration.; Abazajian, K.; et al.. CMB-S4: Forecasting Constraints on Cosmology and Fundamental Physics. *Astrophysical Journal Supplement Series* **2024**, *269*, 45. https://doi.org/10.3847/1538-4365/ad1b03.
31. Simons Observatory Collaboration.; Galitzki, N.; et al.. The Simons Observatory: Science Goals and Forecasts. *Journal of Cosmology and Astroparticle Physics* **2023**, *01*, 056. https://doi.org/10.1088/1475-7516/2023/01/056.